SCIENTIFIC REPORTS
nature research

OPEN

Semimytilus algosus: first known hermaphroditic mussel with doubly uniparental inheritance of mitochondrial DNA

Marek Lubośny✉, Aleksandra Przyłucka, Beata Śmietanka & Artur Burzyński

Doubly uniparental inheritance (DUI) of mitochondrial DNA is a rare phenomenon occurring in some freshwater and marine bivalves and is usually characterized by the mitochondrial heteroplasmy of male individuals. Previous research on freshwater Unionida mussels showed that hermaphroditic species do not have DUI even if their closest gonochoristic counterparts do. No records showing DUI in a hermaphrodite have ever been reported. Here we show for the first time that the hermaphroditic mussel *Semimytilus algosus* (Mytilida), very likely has DUI, based on the complete sequences of both mitochondrial DNAs and the distribution of mtDNA types between male and female gonads. The two mitogenomes show considerable divergence (34.7%). The presumably paternal M type mitogenome dominated the male gonads of most studied mussels, while remaining at very low or undetectable levels in the female gonads of the same individuals. If indeed DUI can function in the context of simultaneous hermaphroditism, a change of paradigm regarding its involvement in sex determination is needed. It is apparently associated with gonadal differentiation rather than with sex determination in bivalves.

Bivalvia is a class of hinge-shell animals, that are broadly used in industry as a food source, pearl producers or diet supplements[1], and have high ecological value as water quality bioindicators[2] and sequesterers of carbon dioxide[3]. They are interesting also in terms of molecular biology. Their byssus proteins[4] (thread-like adhesive structures attaching those animals to the rocky sea bottom) could potentially be used in industry and medicine[5,6]. They are one of the few groups of animals after Tasmanian devils[7], dogs[8] and Syrian hamsters[9] where transmissible cancer was observed[10,11]. Furthermore, many species, more than 100 known so far[12], show doubly uniparental inheritance of mitochondrial DNA (DUI)[13–15], system uniquely different from strict maternal, paternal or biparental inheritance. In DUI two highly divergent, from 10% to over 50%[16], mitochondrial DNA types are present in male individuals. Females are homoplasmic (F-type mtDNA) and males are heteroplasmic (F-type present in somatic tissues and M-type dominating gonads). Progeny receive different types of mitochondria through homoplasmic gametes: F from eggs and M from sperm[17]. Depending on the progeny's sex the mitochondria from the father are either lost (female progeny), or are grouped together, becoming the dominant fraction in the male gonad[18] (male progeny).

With the expanding knowledge on taxonomic distribution of this phenomenon, evolutionary studies try to answer the question of the DUI origin: how many times DUI evolved, whether it is a bivalvian synapomorphy or whether it was lost and re-invented several times independently[14,19,20]. Studies concerning molecular mechanisms involve quests for candidate DUI-related genes in transcriptomes[21,22] primarily focusing on mtDNA-derived sequences, often featuring additional mitochondrial open reading frames (ORF) and extensions of mitochondrial genes[21,23–27]. Studies have shown that these ORFs are indeed transcribed and translated, implying their role in the segregation of mitochondria[27–29]. It has also been suggested that DUI evolved primarily as a sex determination system[30], with the mitogenome influencing the sex of the progeny. Hermaphroditic species of freshwater mussels (Unionoida), lose not only the paternally inherited M mitogenome but also the gender-specific open reading frame in the remaining F type mitogenome. Following this, the hermaphroditic freshwater mussel *Anodonta cygnea* does not have supranumerary open reading frames in the mitogenome[31].

Department of Genetics and Marine Biotechnology, Institute of Oceanology Polish Academy of Sciences, Sopot, Poland. ✉email: lubosny@iopan.pl

Semimytilus algosus (Gould, 1850) is a small, marine mussel living on wave-exposed rocky shores along the Pacific coast of South America as well as on the western (Atlantic) coast of Africa, where it has been marked as an invasive species[32,33]. The species is a simultaneous hermaphrodite with male and female gonads located in the mantle tissues on the opposite sides of the body (different shell halves): the grey-violet mantle contains female gonads and the whitish mantle contains male gonads[34]. As we show in the following article it is the first known hermaphroditic mussel possessing doubly uniparental inheritance, which indicates that DUI is connected with gamete differentiation rather than with sex determination in bivalves.

Results

mtDNA. Two divergent mitogenomes were detected in the male and female gonads of an individual *S. algosus* mussel. Both were sequenced and annotated. We will refer to the mitogenome dominating male gonads as M, and the other as F. The M and F mitogenomes (Fig. 1) differ in length. The F mitogenome is shorter (18,113 bp) than the M mitogenome (24,347 bp). Both mitogenomes encode all genes on a single strand: 13 protein-coding genes, 2 *rRNA* genes, and at least 23 *tRNA* genes were identified, including a second *tRNA* for methionine with TAT anticodon. Despite the length difference, the structure of the coding part is similar. One major difference concerns the small subunit *rRNA* gene. *12S rRNA* in the F genome is located between *nad1* and *cox1* genes whereas in the M mitogenome it is located in the region between the *16S rRNA* and *nad4l* genes. In addition to that, *atp8* in M mitogenome is exceptionally long (885 bp). There is no indication of polyadenylation inside its transcript, which would allow shorter annotation, although the transcript coverage (Table S1) in this region is quite low (8.82 ± 5.07). Minor structural differences between the M and F mitogenomes involve different relative locations of some *tRNA* genes: $tRNA^{Asn}$, $tRNA^{Arg}$ and $tRNA^{Met}$. Finally, the non-coding regions have different length and localization in the two mitogenomes. In the M mitogenome a major non-coding region, very long and rich in repetitive sequences, is located between the two *rRNA* genes whereas in the F mitogenome the longest non-coding region is between $tRNA^{Met}$ and $tRNA^{Asn}$ and does not contain repetitive sequences. There are several other, shorter non-coding regions in both mitogenomes, none with any level of between-genome similarity.

In the F mitogenome two cases of possible duplication of *tRNA* genes were observed. The first case concerns the $tRNA^{Pro}$-like structure located before *nad6.* This gene has a larger p-distance than true $tRNA^{Pro}$ (0.377) but has conserved the anticodon loop structure. The second case concerns $tRNA^{Ser2}$-like sequence located before *atp8* gene. This one has smaller p-distance than true $tRNA^{Ser2}$ (0.147), but anticodon sequence is modified from AGA to AGC. In each of the two cases the polyadenylation signal marks beginning of the *tRNA*-like gene and there is no corresponding sequence in the M mitogenome.

There are several *tRNA*-like genes in the M mitogenome, too. They all involve $tRNA^{Gln}$ or $tRNA^{His}$ specificities. The two possible candidates for $tRNA^{Gln}$ genes: one directly behind *12S rRNA* and the second between $tRNA^{Tyr}$ and $tRNA^{Asn}$, are difficult to differentiate, similar p-distance 0.344 and 0.388 and Gibbs free energy (dG − 9.4 and − 10.4 kcal/mol respectively) for clover leaf structure. Since there is no clear way to discriminate one over another both will be treated as possibly valid *tRNA* genes. Apart from the $tRNA^{His}$ gene located before *cox1,* as in the F mitogenome, there are several $tRNA^{His}$-like structures in repetitive non-coding region of the M mitogenome. Some of them show the most stable structure (lowest dG) but the one before *cox1* gene, the most similar to $tRNA^{His}$ from the F mitogenome (p-distances of 0.571 and 0.339 respectively) has been annotated as the correct one.

We were able to identify the polyadenylation sites (pA) in the F mitogenome, indicating the span of the mature transcripts. All protein and *rRNA* genes produce individual transcripts, except for *atp8* and *atp6*, which apparently form a bicistronic transcript. Unfortunately, for the M mitogenome RNA-seq coverage was much lower and only few pA sites were detected: after *16S rRNA* before long repetitive region, after repetitive region before *12S rRNA* and at boundaries of some *tRNA* genes (Fig. 1).

Divergence and phylogenetics. The overall divergence (p-distance) between F and M genomes (Fig. 2) is quite high (0.347) achieving an unusually high value for cox3 protein, almost two times higher than for the F and M genomes of *Perumytilus purpuratus*. Beside this protein, *12S rRNA*, atp8 and nad2 pairs are slightly more divergent in *S. algosus* than their counterparts in other known DUI possessing mytilids. Nevertheless, in the phylogenetic reconstruction (Fig. 3) the separation of F and M lineages in *S. algosus* is more recent than in *Geueknsia demissa* or *Perumytilus purpuratus* even though their overall M to F divergence (p-distance) is lower then for *S. algosus*. This is because the evolutionary rate in the M lineage of *S. algosus* is substantially higher than that of other mytilids, indicated here by values on phylogenetic tree branches.

To ascertain the intrapopulation divergence and compare selective pressure acting on F and M mitogenomes, three fragments from each mitogenome from eighteen individuals were amplified and sequenced (Table 1). A higher level of polymorphism has been observed for the genes from the F mitogenome. The ratios of non-sysonymous and synonymous substitutions and polymorphisms suggest strong purifying selection acting on both mitogenomes.

qPCR. The distribution of the M and F mitogenomes in gonads/mantles (gonads and mantles are inseparably connected) was measured by qPCR with relation to a single-copy nuclear gene (Fig. 4). The M mitogenome was present in appreciable concentrations only in male gonads, although the exact value varied. The ratios of M to F concentrations were also calculated (Fig. 5). There is from hundreds, up to more than ten thousand times more F-type mtDNA than M-type mtDNA in female mantles, and, excluding the four cases, there was from three to twelve times more M-type mtDNA than F-type mtDNA in male mantle tissues. The four exceptional cases had more F-type mtDNA in the male mantle tissue, but only up to 30 times more. In the male gonad of individual PL02M, which apparently has the smallest M/F ratio in male mantle, it was estimated at 27.59 (CI: 25.03–30.42).

The same tissue sample was used in next generation sequencing (NGS), and the ratio derived from sequencing the data was 31.05 (26.77–36.18), in good agreement with the qPCR estimate.

Due to the lack of live specimens there was no possibility to check the precise mtDNA content in separated and purified sperm cells. In this species mantle tissues contain both somatic and generative cells. As a result, assuming that sperm cells are homoplasmic[15,35,36] for M-type mtDNA, and that F-type mtDNA in mantle represent somatic cells' contribution, estimation of the mtDNA content in spermatozoa is possible. The plot of M-mtDNA/nDNA in the male mantle against F-mtDNA/nDNA in the same tissue (qPCR data) extrapolated to the zero should give an estimate of the M-mtDNA/nDNA ratio of pure sperm. The result is a straight trend line showing reasonably high correlation $R^2 = 0.9238$ (Fig. 6) and crossing the Y axis at 15.06 (14.11- 16.26). It means that each sperm cell contains approximately 15 copies of M-mtDNA. Assuming that there are five mitochondria per sperm cell[18,37], there should be around three M-mtDNA molecules in each sperm mitochondrion.

Discussion

The two mitogenomes isolated from *S. algosus* both show a fairly typical structure. There were only minor difficulties with the certainty of some *tRNA* gene annotations, otherwise the complete set of metazoan mtDNA encoded genes was unambiguously identified in both. Based on the phylogenetic analysis (Fig. 3) the possibility that one of the mitogenomes comes from a contaminating, unrelated organism can safely be discarded: the two mitogenomes, despite the substantial genetic distance, form a sister relationship on the tree. Moreover, there are only a few structural differences between them, which could be explained by translocations involving primarily *12S rRNA* and three *tRNA* genes. A similar amount of structural differences between M and F mitogenomes is known in freshwater mussels[28], but was not reported from a mytilid bivalve so far.

DUI is often associated with lineage-specific features present in the mitogenomes. With this respect, the presence of the very long *atp8* gene in M mitogenome is a possible candidate in *S. algosus*. This gene does vary in length in bivalves but in *S.algosus* it is extreme: over two times longer than in *Mytilus*[38–40]. Moreover, few 7–9 amino acid long repeats are present at the C-end of the hypothetical protein (Fig. S1). This gene extension could potentially be involved in mitochondria tagging mechanism, as postulated for similar extensions in other DUI bivalves[24,25,28,29,41–43]. Additional open reading frames (ORFs), as well as mitochondrial sequence coverage with RNA transcripts have been marked on supplementary Fig. 2 (Fig. S2). With gathered data it is hard to speculate about possible involvement of those ORFs in mitochondrial DNA inheritance.

All other genes have similar length. With one exception they also follow a similar pattern of divergence (Fig. 2). The exceptionally divergent cox3 (nearly 60% p-distance at amino acid level) is located close to an AT-rich region in both mitogenomes, and must have been involved in translocation events. These could explain the increased relative mutational pressure, but the observed genetic distance could also be a result of metabolic remodelling, recently shown to involve OXPHOS complexes IV and V in DUI bivalves[44].

Reported amounts of mtDNA copies per cell[45–47] vary greatly in different organisms, cell types and stages of oogenesis, from less than one thousand to hundreds of thousends[46,47]. For bivalves information about mtDNA copy number is scarce and indirect[36,48,49], but the high concentrations of F-mtDNA in the female mantle observed in *S. algosus* are not surprising. The expectation from DUI model would be the exclusive presence of M mtDNA in sperm and ubiquitous presence of F mtDNA in other tissues[15,35,36]. We observed marked differences between individuals, particularly with respect to F mtDNA content in male mantle (Fig. 4). These may represent different stages of gametogenesis or different extents of contribution from the adjacent somatic tissues, in agreement with the model. The M-type mtDNA was consistently present in male mantle (29.2 ± 15.7 copies per nuclear genome). Very similar values were reported from male gonads of *Venerupis philippinarum* (32.25 ± 16.63)[36]. Even if the differences in the anatomy of these bivalves and the different choice of the reference gene make direct comparison of these results difficult, they do fulfill the expectation of the DUI model. The occasional presence of M-mtDNA in the female mantle is more problematic. It is commonly assumed that females and somatic tissues in DUI males are free from M-type mtDNA[50], but depending on the individual species and molecular technique used, exceptions to this rule were also shown[36,51]. In the case of the hermaphroditic *S. algosus,* M-type mtDNA is always present in one of their mantles, so the contamination with small amounts of M-mtDNA is apparently difficult to avoid. The detected concentrations were always very low, consistent with this view.

To ascertain the possibility that the observed mitochondrial sequences represent *numts* rather than true mitogenomes, the polymorphisms of both mitogenomes were measured at a population level. At this level mitochondrial genes show a strong signature of purifying selection, evidenced by omega values much smaller than one[52]. For the two representative fragments of both *S. algosus* mitogenomes the observed polymorphism was also consistent with strong purifying selection (Table 1), supporting the view that these sequences are not *numts*. The overall level of polymorphism was very low, particularly in the M data set. The M mitogenome usually shows higher polymorphism than the F mitogenome[42,53] especially for larger data sets[52,54], but there is a known case of the mytilid *Musculista senhousia*[41], where the situation is opposite. These anomalies can be explained by compensation draft feedback (CDF) process acting on the DUI tripartite genome, with more frequent selective sweeps in the M lineage periodically lowering its polymorphism[39]. Consequently, the evolutionary rates are higher for the M lineages than for the corresponding F lineages (Fig. 3).

The presented arguments show that the two divergent mitogenomes of *S. algosus* are part of the DUI system. Consequently, it can be concluded that hermaphroditic bivalves can have the DUI system and that this system is associated with gonad development, rather than sex determination. The number of M-mtDNA copies present in a single sperm cell of *S. algosus*, was estimated at approximately 3 (Fig. 6). This number is in good agreement with the estimates of 1 up to 10 reported in mammals[45,55,56]. Our estimate may not be very precise, but the error should not exceed one copy per mitochondrion. The overall linear relationship between the M- and F- mtDNA concentration in the male mantle is intriguing. In DUI animals, the fate of paternal mtDNA in zygotes has been

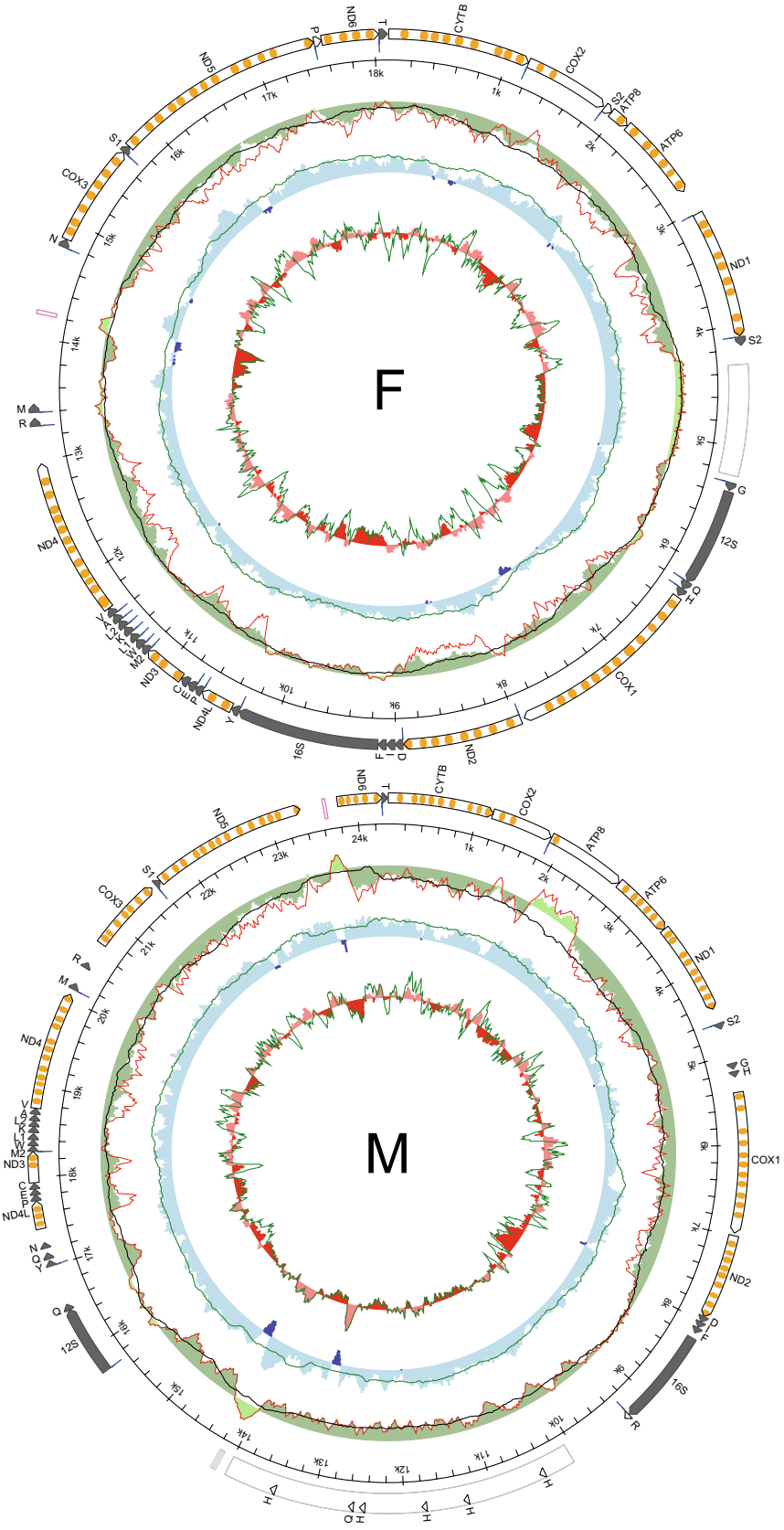
F
M
NDG
T
CYTB
COX2
S2
ATP8
ATP6
ND1
S2
G
12S
H
COX1
ND2
I
D
16S
F
ND4L
Y
ND3
M2
ND4
R
M
COX3
S1
ND5
P

◂**Figure 1.** Genetic map of *Semimytilus algosus* mitochondrial genomes. The white arrows represent protein coding genes with predicted transmembrane domains of encoded proteins marked in orange. The long dark arrows represent rRNA genes; the short dark arrows represent tRNA labeled by a one letter amino acid code, short white arrows represent duplicated tRNA-like structures, a pink box indicates the location of an AT-rich region; a grey box indicates the location of repetitive sequences; blue lines in front of the genes show the location of the polyadenylation signal. Inner circles represent local compositional bias, calculated in a 200 bp long sliding window with 25 bp steps, unless indicated otherwise. A green outer circle represents a AT-skew (A−T/A+T); a red line represents a filtered AT-skew, calculated at non-coding regions and the second codon position only. A black line represents a filtered AT-skew, calculated at neutral and non-coding positions only, in a larger, 1000 bp long window. A middle blue circle represents a GC skew (G−C/G+C), and a green line represents a GC skew at neutral sites, calculated in a window of 1,000 bp. Both skew indices are presented in absolute scale, starting at zero. An inner red circle represents local GC content, and a green line shows GC content at neutral sites. Local GC content is presented in scale relative to the average for the whole mitogenome.

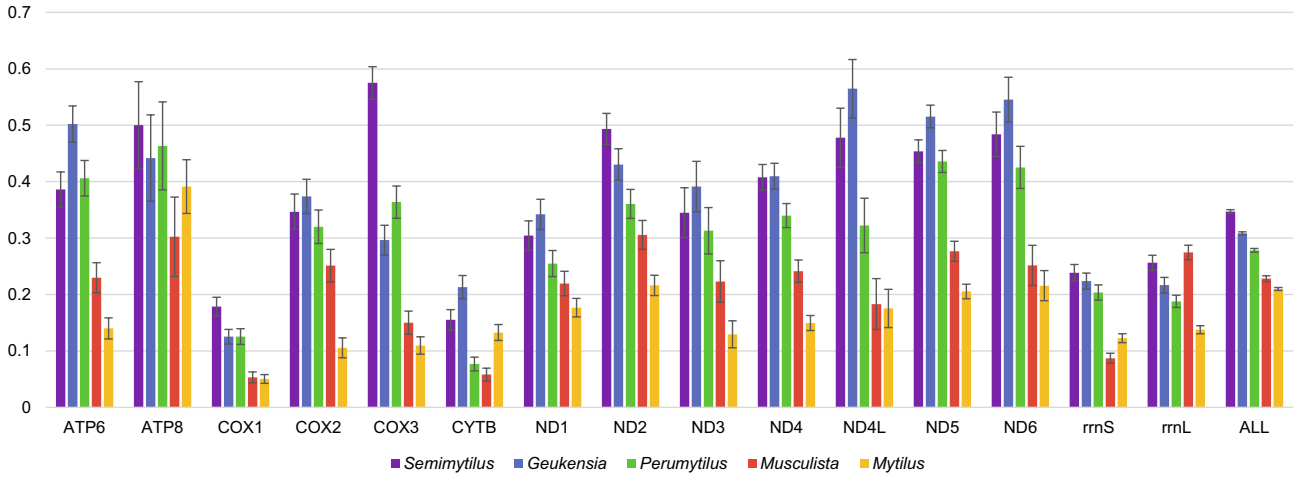

Figure 2. Average distance (p-distance) between protein and gene sequences from M and F genomes in Mytilidae. Violet bars represent *Semimytilus algosus*, blue bars represent *Geukensia demissa* (two genomes), green bars represent *Perumytilus purpuratus* (four genomes), red bars represent *Musculista senhousia* (two genomes), and yellow bars represent the *Mytilus edulis* complex (six genomes). Each gene sequence was extracted and aligned separately. The average between-group nucleotide p-distance was calculated in MEGA7. Standard error estimates were calculated by bootstrap procedure (10,000 replicates). For protein coding genes, amino acid p-distances are shown; for RNA genes and the overall distance, the nucleotide p-distances are shown.

tracked through the first stages of development[18,57–59]. At these early stages, the advantage of F-type mtDNA is overwhelming in all cells, even those containing M-type mtDNA. Despite that, there is no F-type mtDNA in sperm, only M-type is present there. It has been suggested previously, that this elimination is a competitive process, possibly mediated by replicative advantage of M-type mtDNA over F-type mtDNA[60–62]. Our results suggest that the dominance of M mitogenome in sperm is achieved by a mild stepwise process and does not involve sudden expansion of the M-mitogenome. Further studies, involving other tissues and developmental stages should clarify this. *S. algosus* appears to be a perfect model system for DUI research as each individual has both mitogenomes, essentially eliminating the sex factor inherent to all previous DUI studies. These should ultimately allow identification of molecular pathways involved in mitochondria inheritance in DUI bivalves and a better understanding of mitochondrial inheritance in general.

Methods

Semimytilus algosus specimens were collected in January 2014 at the Chilean Pacific coast (33°29′09.60″S, 71°38′40.97″W). The presence of male and female gonads was determined by mantle tissue examination under light microscopy. Sectioned gonad tissues were suspended in 70% Ethyl alcohol and stored in − 80 °C until further use. RNA and DNA was extracted according to the methods established earlier[63–65]. Tissue samples for DNA extraction (~ 60 mg) were incubated overnight in a 700 µl CTAB extraction buffer (2% CTAB, 0.1 M Tris-HCl, 1.4 M NaCl, 20 mM EDTA, 1 mg/ml proteinase K and 35 mM 2-mercaptoethanol) followed by triple chloroform extraction (1:1 vol/vol) and centrifugation (20,000×*g* for 10 min). Next, the aqueous phase was mixed with cold isopropanol (1:1 vol/vol) and centrifugated again (20,000×*g* for 30 min 4 °C). Retained DNA pellets were washed two times with 75% ethyl alcohol and dried in a vacuum concentrator (60 °C, 15 min). Isolated DNA were resuspended in a Tris-EDTA buffer and the concentrations were measured on a Epoch Microplate Spectrophotometer. RNA was extracted with GenElute Mammalian Total RNA Miniprep Kit (Sigma) optimized for mussel tissues, e.g. the original extraction buffer was exchanged for a CTAB extraction buffer. RNA Integrity was measured in a Epoch Microplate Spectrophotometer (A260/A280 ratio) and by gel electrophoresis.

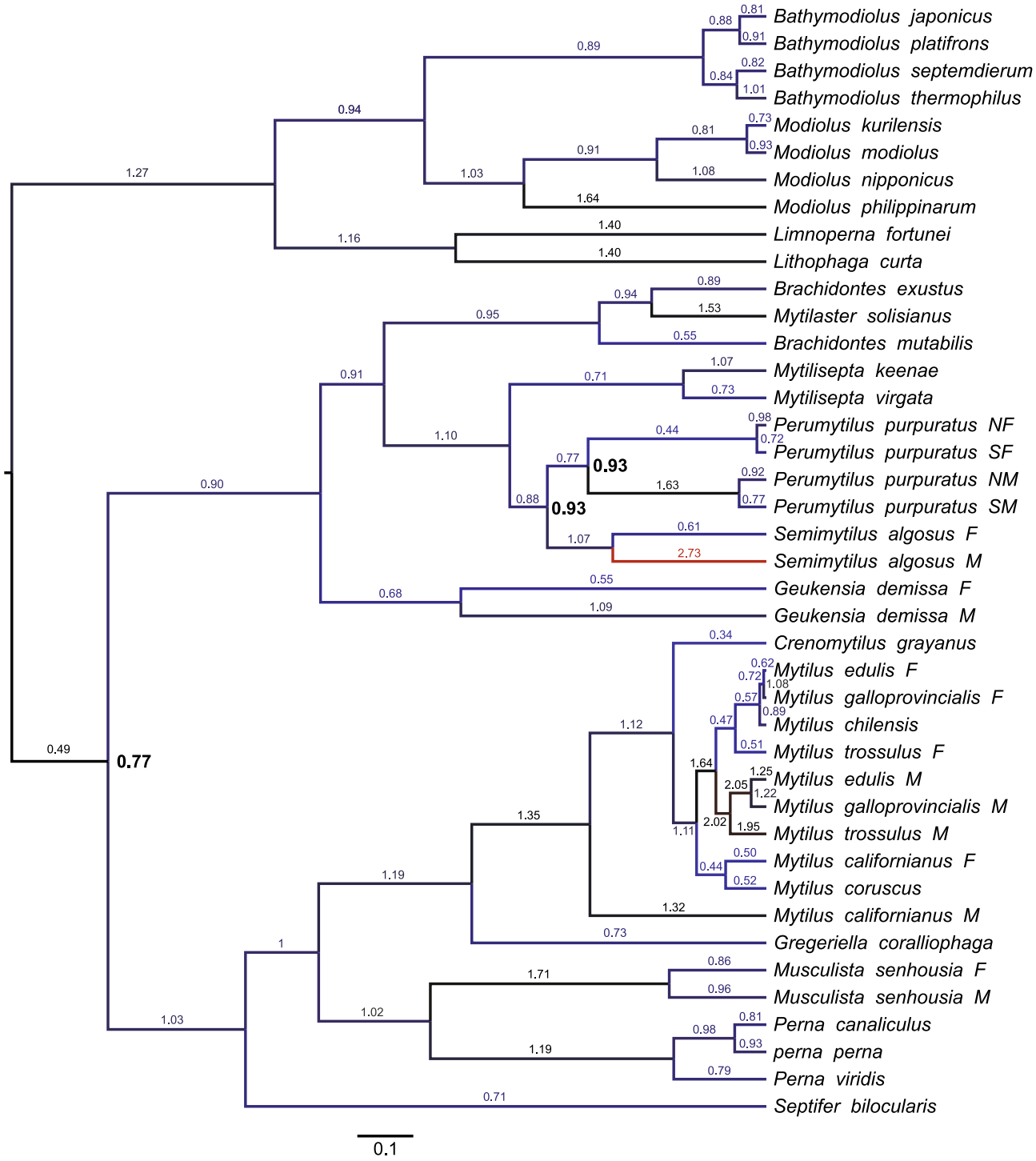

Figure 3. The phylogenetic position of *Semimytilus algosus* mitogenomes among mitogenomes of other mytilid mussels. Posterior probabilities of all bipartitions were 1.0, except for the nodes indicated by the bolded number. Numbers on branches represent evolutionary substitution rate.

Pooled total RNA extracts from three individuals (only male mantle) were then sent to Macrogen Inc. for high throughput sequencing (MiSeq Illumina, TruSeq NGS library 2 × 150 bp). Similarly, total DNA from single male mantle extract was sent for sequencing (HiSeq-X Ten Illumina, TruSeq NGS library 2 × 150 bp). Raw reads are available in the SRA GenBank database under the following accession numbers: SRR11805503, SRR11809905.

Raw reads after RNA sequencing were then processed and assembled according to the Oyster River protocol[66] and the methodology published earlier[42,65,67]. ABySS[68] was used as a nuclear genome assembler as well as NOVOplasty[69], to pull out and assemble mitochondrial genomes from raw DNA reads. Sequences of assembled mtDNA were then verified by mapping of mitochondrial reads filtered with Bowtie2[70] to the mitogenomes in CLC Genomics Workbench 9.5 (QIAGEN). Both acquired mitogenomes were then annotated following established

mt genome	Region	N	h	S	hd	θ	π	Tajima's D	Ka	S.E	Ks	S.E	Ka/Ks
F	ND5	18	18	111	1.00	0.0247	0.0156	−1.5538	0.0009	0.0004	0.0643	0.0069	0.0140
F	ND6	18	18	34	1.00	0.0251	0.0137	−1.8459*	0.0018	0.0009	0.0529	0.0106	0.0340
F	CYTB	18	18	43	1.00	0.0202	0.0100	−2.0707*	0.0002	0.0002	0.0414	0.0065	0.0048
F	ND5, ND6, CYTB (concatamer)	18	18	188	1.00	0.0235	0.0137	−1.7692	0.0009	0.0002	0.0558	0.0047	0.0161
M	ND5	18	8	17	0.83	0.0038	0.0032	−0.5852	0.0003	0.0003	0.0122	0.0035	0.0246
M	ND6	18	6	6	0.78	0.0042	0.0045	0.2480	0.0004	0.0003	0.0175	0.0083	0.0229
M	CYTB	18	5	10	0.71	0.0044	0.0059	1.2481	0.0000	0.0000	0.0242	0.0083	0.0000
M	ND5, ND6, CYTB (concatamer)	18	9	33	0.86	0.0040	0.0042	0.1626	0.0002	0.0002	0.0164	0.0033	0.0122

Table 1. Standard indices of genetic diversity in the coding sequences of ND5 (1,317 bp), ND6 (417 bp) and CYTB (663 bp) region and in the concatenated set of ND5, ND6, CYTB sequences for *Semimytilus algosus* mussel. N—represent the number of individuals, h—the number of identified haplotypes, S—the number of segregating sites, hd—haplotype diversity, θ—number of segregation sites in sample of N DNA sequences, π—nucleotide diversity, Tajima's D—neutrality test, *—represent statistical significance for $p < 0.05$, Ka—nonsynonymous substitutions, Ks—synonymous substitutions.

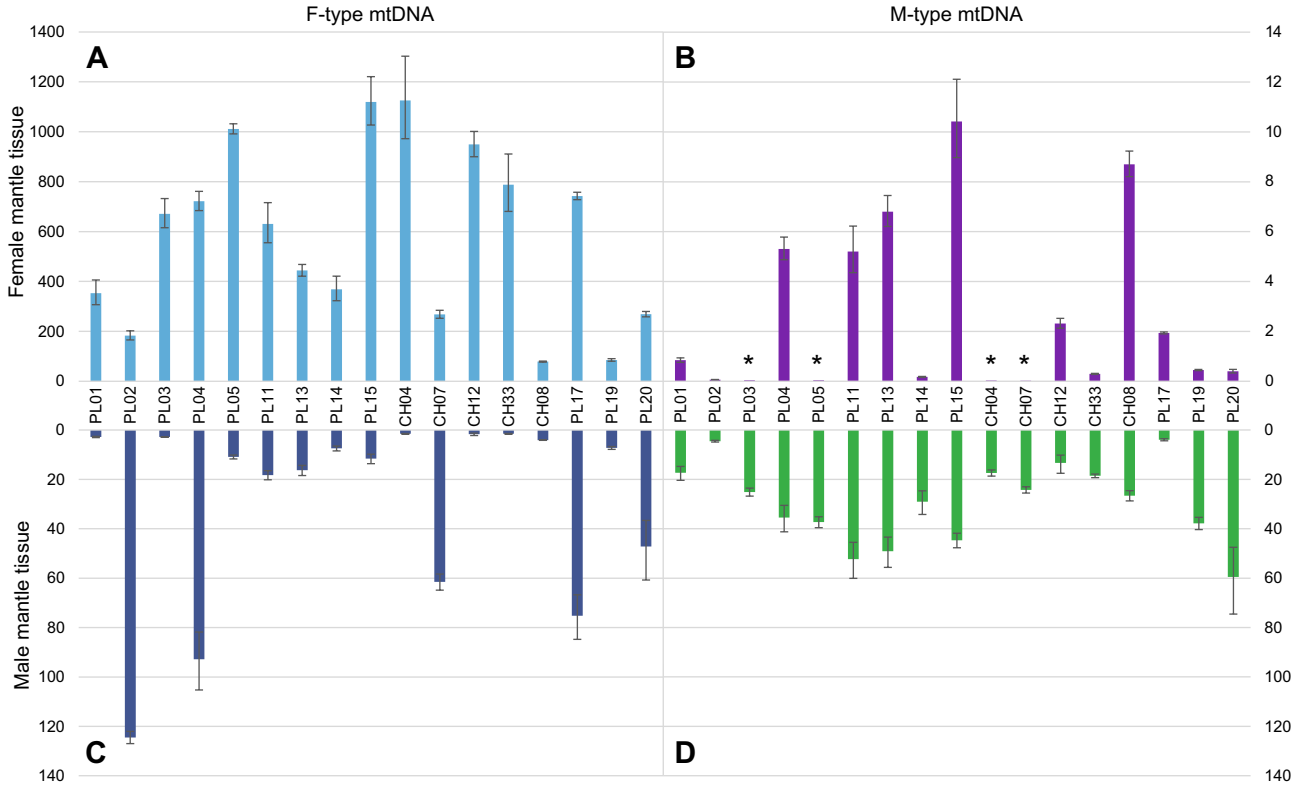

Figure 4. Number of mitochondrial genomes (F *cox1* and M *nad1*) in relation to copies of nuclear DNA (*atpα*). A. F mtDNA to nuclear DNA ratio in the Female mantle; B. M mtDNA to nuclear DNA ratio in the Female mantle; C. F mtDNA to nuclear DNA ratio in the Male mantle; D. M mtDNA to nuclear DNA ratio in theMale mantle. * asterisks show samples where the M mtDNA copy number approaches zero.

workflow[42,71]. Proteins were predicted with CRITICA[72], Wise2[73] and GLIMMER[74]. Ribosomal genes (*tRNAs* and *rRNAs*) were identified with Infernal[75], ARWEN[76] and nhmmer[77]. The location of transmembrane protein domains was predicted with a Phobius[78]. A custom Biopython script was used to calculate compositional indices, synchronize the annotations and draw circular mitochondrial diagrams (https://github.com/aburzynski/mitoconstrictor). More details about the bioinformatic pipeline can be found in the supplementary materials. The annotated features were then verified manually in CLC Genomics Workbench 9.5. Annotated mitochondrial sequences of *Semimytilus algosus* are available in the GenBank database under accession numbers MT026712 and MT026713.

To identify the allelic coverage of the nuclear genome, Jellyfish[79] analyses were performed. K-mer coverage values between the homozygous and heterozygous peaks (2N-1N alleles) were set for target single copy nuclear

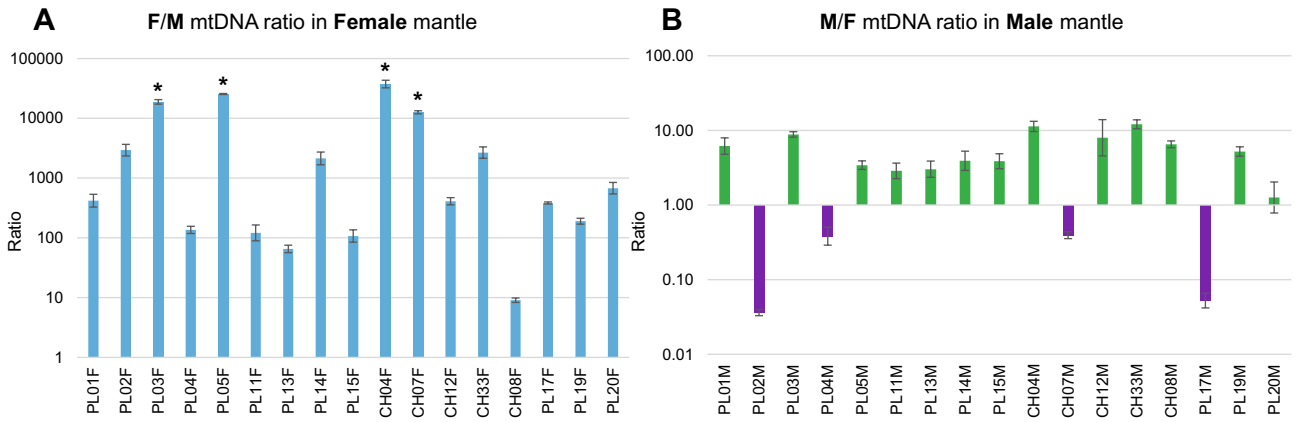

Figure 5. Ratios of M to F and F to M mitogenomes in tissues. A. F to M mtDNA ratio in Female mantle issues; B. M to F mtDNA ratio in Male mantle; * asterisks show samples where the M mtDNA copy number approaches zero, hence in those samples the F/M ratio lies between infinity and the marked value. All results were presented in logarithmic scale.

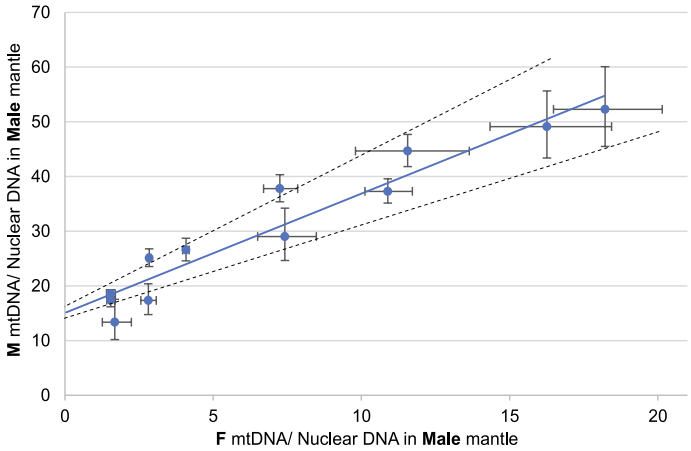

Figure 6. The correlation of the M and F mtDNA copy number in male tissues based on qPCR results. Intersection of the regression line with the Y axis marks predicted copy number of M mitogenomes in single sperm cell. Dotted line shows standard deviation.

gene identification (Fig. S3). This was performed in order to exclude genes with more than two alleles which would indicate the existence of more than one gene copy. Nuclear genes were chosen by non-random method: pick a known gene annotated in *Crassostrea gigas* (GCA_000297895.1) genome[80,81], search it with BLAST[82] and Wise2[73] for its counterpart in *Semimytilus algosus* transcriptome, then map identified transcripts onto the *S. algosus* assembled genome. Filter out mapped reads with Bowtie2[70] and check the k-mer coverage (repeat until a suitable gene is identified). Two pairs of nuclear primers and six pairs of mitochondrial (3 pairs for F and 3 pairs for M mtDNA) primers were designed in Primer3[83] for a qPCR reaction. As a result of primer optimisation (Efficiency between 90 and 110%) only three pairs of primers remained (Nuclear: *ATP asynthase alpha subunit*, F mtDNA: *cox1*, M mtDNA: *nad1*). Primers for the F and M-type mitogenomes were experimentally checked to ensure no amplification of homologous sequences from the second mitogenome. For every gene a freshly diluted standard curve (PCR amplified template spanning gene of interest) was run along the samples and a non template control. The final standard curve was established as an average for three experiments (3 experiments × 3 replicates × 7 folds of dilution).

QPCR reactions verifying amounts of F and M mtDNA in tissues were performed on a ECO48 (Illumina) Real Time PCR System according to protocol supplied by the manufacturer (EURx): a reaction volume of 10 µl per sample, 1 × SG qPCR Master Mix, 2 µl of DNA concentration ~ 11 ng/µl linearized with a NdeI restriction enzyme, 0.5 µM of primers. Thermal profile: initial denaturation 95 °C for 10 min followed by 35 cycles of denaturation 10 s 94 °C, annealing 60 °C 30 s, elongation 72 °C 30 s, melt curve 55–95 °C. Primers sequences and raw results are available in Table S4–S7.

Phylogenetic reconstruction of the Mytilidae family[67,84] were performed in BEAST2[85] on 12 mitochondrial protein sequences (Fig. 3). Complete mitochondrial genomes of 41 individuals (8 F/M pairs and 32 species) were downloaded from the GenBank database in November 2019 (Table 2). MEGA7[86] has been used for sequence

Species and references	Acc. No	Species and references	Acc. no
Bathymodiolus japonicus[88]	AP014560	*Mytilus californianus* F[89]	GQ527172
Bathymodiolus platifrons[88]	AP014561	*Mytilus californianus* M[89]	GQ527173
Bathymodiolus septemdierum[88]	AP014562	*Mytilus chilensis*[90]	KT966847
Bathymodiolus thermophilus[84]	MK721544	*Mytilus coruscus*[91]	KJ577549
Brachidontes exustus[92]	KM233636	*Mytilus edulis* F[38]	MF407676
Brachidontes mutabilis[84]	MK721541	*Mytilus edulis* M[93]	HM489874
Crenomytilus grayanus[84]	MK721543	*Mytilus galloprovincialis* F[94]	FJ890850
Geukensia demissa F[67]	MN449487	*Mytilus galloprovincialis* M[94]	FJ890849
Geukensia demissa M[67]	MN449488	*Mytilus trossulus* F[39]	HM462080
Gregeriella coralliophaga[84]	MK721545	*Mytilus trossulus* M[39]	HM462081
Limnoperna fortunei[95]	KP756905	*Perna canaliculus*[96]	MG766134
Lithophaga curta[84]	MK721546	*Perna perna*	(unpublished)
Modiolus kurilensis	KY242717	*Perna viridis*[97]	JQ970425
Modiolus modiolus[98]	KX821782	*Perumytilus purpuratus* NF[42]	MH330322
Modiolus nipponicus[84]	MK721547	*Perumytilus purpuratus* NM[42]	MH330330
Modiolus philippinarum[99]	KY705073	*Perumytilus purpuratus* SF[42]	MH330333
Musculista senhousia F[41]	GU001953	*Perumytilus purpuratus* SM[42]	MH330331
Musculista senhousia M[41]	GU001954	*Semimytilus algosus* F	MT026712
Mytilaster solisianus[100]	KM655841	*Semimytilus algosus* M	MT026713
Mytilisepta keenae[84]	MK721542	*Septifer bilocularis*[84]	MK721549
Mytilisepta virgata[84]	MK721548		

Table 2. List of mitogenomes used in phylogenetic analyses, with species, lineage, accession numbers, and references (wherever available).

alignment and p-distance divergence calculations. Protein sequences were aligned using ClustalW algorithm with Gap Extension and Gap Opening cost set at 5. Parameters for phylogenetic analysis were as follows: mtREV model, relaxed log-normal clock and Yule prior to the common tree. Markov chain was run in four replicates for 10^7 generations and sampled every 10,000th step. Convergence of samples was checked with Tracer[87], effective sample size for estimated parameters was greater than 200.

Two sets of primers covering fragments of the three genes have been designed[83] to evaluate selective pressure (Table 1) acting on F and M-type mtDNA. DNA from 18 pairs of female and male mantle tissue samples was extracted using a modified CTAB protocol[63]. PCR amplifications were carried out in a 12 µl reaction volume with approximately 5 ng of total DNA, 0.5 µM each primer, dNTPs at 200 µM each, 0.02 U/µl of Phusion DNA Polymerase (Thermo Fisher Scientific) in a GC buffer supplied by the manufacturer. The TProfessional Thermocycler (Biometra) was used to perform amplification reactions according to the following protocol: 30 s at 98 ˚C initial denaturation, 30 cycles of denaturation for 10 s at 98 ˚C, annealing for 30 s at temperature dependent on primers (Table S8) and extension for 45 s at 72 ˚C. The final extension lasted 10 min. Amplified products where then sent for sequencing to Macrogen Inc. (Korea). The Gap4 software from the Staden package version 1.7.0[101] was used to assemble sequences. Alignments and sequence analysis were performed using MEGA7[86] and DnaSP[102] software. The nucleotide divergences of protein genes in synonymous (Ks) and non-synonymous sites (Ka) using the Nei–Gojobori method with Jukes–Cantor correction were calculated in MEGA7. The calculations of the D test statistic proposed by Tajima[103] was performed in DnaSP[102].

Received: 23 March 2020; Accepted: 11 June 2020
Published online: 09 July 2020

References

1. Cobb, C. S. & Ernst, E. Systematic review of a marine nutriceutical supplement in clinical trials for arthritis: the effectiveness of the New Zealand green-lipped mussel *Perna canaliculus*. *Clin. Rheumatol.* **25**, 275–284 (2006).
2. Waykar, B. & Deshmukh, G. Evaluation of bivalves as bioindicators of metal pollution in freshwater. *Bull. Environ. Contam. Toxicol.* **88**, 48–53 (2012).
3. Filgueira, R. *et al.* An integrated ecosystem approach for assessing the potential role of cultivated bivalve shells as part of the carbon trading system. *Mar. Ecol. Prog. Ser.* **518**, 281–287 (2015).
4. Duarte, A. P., Coelho, J. F., Bordado, J. C., Cidade, M. T. & Gil, M. H. Surgical adhesives: Systematic review of the main types and development forecast. *Prog. Polym. Sci.* **37**, 1031–1050 (2012).
5. Santonocito, R. *et al.* Recombinant mussel protein Pvfp-5β: a potential tissue bioadhesive. *J. Biol. Chem.* **294**, 12826–12835 (2019).
6. Dove, J. & Sheridan, P. Adhesive protein from mussels: possibilities for dentistry, medicine, and industry. *J. Am. Dent. Assoc. 1939* **112**, 879 (1986).
7. Epstein, B. *et al.* Rapid evolutionary response to a transmissible cancer in Tasmanian devils. *Nat. Commun.* **7**, 1–7 (2016).
8. Murchison, E. P. *et al.* Transmissible dog cancer genome reveals the origin and history of an ancient cell lineage. *Science* **343**, 437–440 (2014).

9. Ashbel, R. Spontaneous transmissible tumours in the syrian hamster. *Nature* **155**, 607–607 (1945).
10. Metzger, M. J., Reinisch, C., Sherry, J. & Goff, S. P. Horizontal transmission of clonal cancer cells causes leukemia in soft-shell clams. *Cell* **161**, 255–263 (2015).
11. Metzger, M. J. *et al.* Widespread transmission of independent cancer lineages within multiple bivalve species. *Nature* **534**, 705–709 (2016).
12. Gusman, A., Lecomte, S., Stewart, D. T., Passamonti, M. & Breton, S. Pursuing the quest for better understanding the taxonomic distribution of the system of doubly uniparental inheritance of mtDNA. *PeerJ* **4**, e2760 (2016).
13. Zouros, E., Oberhauser Ball, A., Saavedra, C. & Freeman, K. R. An unusual type of mitochondrial DNA inheritance in the blue mussel *Mytilus*. *Proc. Natl. Acad. Sci. U. S. A.* **91**, 7463–7467 (1994).
14. Hoeh, W. R., Stewart, D. T., Sutherland, B. W. & Zouros, E. Multiple origins of gender-associated mitochondrial DNA lineages in bivalves (Mollusca: Bivalvia). *Evolution* **50**, 2276–2286 (1996).
15. Skibinski, D. O., Gallagher, C. & Beynon, C. M. Sex-limited mitochondrial DNA transmission in the marine mussel *Mytilus edulis*. *Genetics* **138**, 801–809 (1994).
16. Doucet-Beaupré, H. *et al.* Mitochondrial phylogenomics of the Bivalvia (Mollusca): Searching for the origin and mitogenomic correlates of doubly uniparental inheritance of mtDNA. *BMC Evol. Biol.* **10**, 50 (2010).
17. Breton, S., Beaupré, H. D., Stewart, D. T., Hoeh, W. R. & Blier, P. U. The unusual system of doubly uniparental inheritance of mtDNA: Isn't one enough?. *Trends Genet. TIG* **23**, 465–474 (2007).
18. Obata, M. & Komaru, A. Specific location of sperm mitochondria in mussel *Mytilus galloprovincialis* zygotes stained by MitoTracker. *Dev. Growth Differ.* **47**, 255–263 (2005).
19. Passamonti, M. & Ghiselli, F. Doubly uniparental inheritance: two mitochondrial genomes, one precious model for organelle DNA inheritance and evolution. *DNA Cell Biol.* **28**, 79–89 (2009).
20. Ladoukakis, E. D. & Zouros, E. Evolution and inheritance of animal mitochondrial DNA: rules and exceptions. *J. Biol. Res.* **24**, 2 (2017).
21. Mitchell, A., Guerra, D., Stewart, D. & Breton, S. In silico analyses of mitochondrial ORFans in freshwater mussels (Bivalvia: Unionoida) provide a framework for future studies of their origin and function. *BMC Genomics* **17**, 597 (2016).
22. Capt, C., Renaut, S., Stewart, D. T., Johnson, N. A. & Breton, S. Putative mitochondrial sex determination in the bivalvia: Insights from a hybrid transcriptome assembly in freshwater mussels. *Front. Genet.* **10**, 840 (2019).
23. Curole, J. P. & Kocher, T. D. Ancient sex-specific extension of the cytochrome c oxidase II gene in bivalves and the fidelity of doubly-uniparental inheritance. *Mol. Biol. Evol.* **19**, 1323–1328 (2002).
24. Chakrabarti, R. *et al.* Presence of a unique male-specific extension of C-terminus to the cytochrome c oxidase subunit II protein coded by the male-transmitted mitochondrial genome of *Venustaconcha ellipsiformis* (Bivalvia: Unionoidea). *FEBS Lett.* **580**, 862–866 (2006).
25. Minoiu, I., Burzyński, A. & Breton, S. Analysis of the coding potential of the ORF in the control region of the female-transmitted *Mytilus* mtDNA. *Gene* **576**, 586–588 (2016).
26. Kyriakou, E., Chatzoglou, E., Rodakis, G. C. & Zouros, E. Does the ORF in the control region of *Mytilus* mtDNA code for a protein product?. *Gene* **546**, 448–450 (2014).
27. Milani, L., Ghiselli, F., Maurizii, M. G., Nuzhdin, S. V. & Passamonti, M. Paternally transmitted mitochondria express a new gene of potential viral origin. *Genome Biol. Evol.* **6**, 391–405 (2014).
28. Breton, S. *et al.* Comparative mitochondrial genomics of freshwater mussels (Bivalvia: Unionoida) with doubly uniparental inheritance of mtDNA: gender-specific open reading frames and putative origins of replication. *Genetics* **183**, 1575–1589 (2009).
29. Ouimet, P. *et al.* The ORF in the control region of the female-transmitted *Mytilus* mtDNA codes for a protein. *Gene* **725**, 144161 (2020).
30. Breton, S. *et al.* Novel protein genes in animal mtDNA: A new sex determination system in freshwater mussels (Bivalvia: Unionoida)?. *Mol. Biol. Evol.* **28**, 1645–1659 (2011).
31. Soroka, M. & Burzyński, A. Hermaphroditic freshwater mussel *Anodonta cygnea* does not have supranumerary open reading frames in the mitogenome. *Mitochondrial DNA Part B* **2**, 862–864 (2017).
32. Tokeshi, M. & Romero, L. Filling a gap: Dynamics of space occupancy on a mussel-dominated subtropical rocky shore. *Mar. Ecol. Prog. Ser.* **119**, 167–176 (1995).
33. de Greef, K., Griffiths, C. L. & Zeeman, Z. Deja vu? A second mytilid mussel, *Semimytilus algosus*, invades South Africa's west coast. *Afr. J. Mar. Sci.* **35**, 307–313 (2013).
34. Bigatti, G., Signorelli, J. & Schwindt, E. Potential invasion of the Atlantic coast of South America by *Semimytilus algosus* (Gould, 1850). *BioInvasions Rec.* **3**, 241–246 (2014).
35. Venetis, C., Theologidis, I., Zouros, E. & Rodakis, G. C. No evidence for presence of maternal mitochondrial DNA in the sperm of *Mytilus galloprovincialis* males. *Proc. R. Soc. B Biol. Sci.* **273**, 2483–2489 (2006).
36. Ghiselli, F., Milani, L. & Passamonti, M. Strict sex-specific mtDNA segregation in the germ line of the DUI species *Venerupis philippinarum* (Bivalvia: Veneridae). *Mol. Biol. Evol.* **28**, 949–961 (2011).
37. Longo, F. J. & Dornfeld, E. J. The fine structure of spermatid differentiation in the mussel, *Mytilus edulis*. *J. Ultrastruct. Res.* **20**, 462–480 (1967).
38. Lubośny, M., Przyłucka, A., Śmietanka, B., Breton, S. & Burzyński, A. Actively transcribed and expressed *atp8* gene in *Mytilus edulis* mussels. *PeerJ* **6**, e4897 (2018).
39. Smietanka, B., Burzyński, A. & Wenne, R. Comparative genomics of marine mussels (Mytilus spp.) gender associated mtDNA: Rapidly evolving *atp8*. *J. Mol. Evol.* **71**, 385–400 (2010).
40. Breton, S., Stewart, D. T. & Hoeh, W. R. Characterization of a mitochondrial ORF from the gender-associated mtDNAs of Mytilus spp. (Bivalvia: Mytilidae): Identification of the 'missing' ATPase 8 gene. *Mar. Genomics* **3**, 11–18 (2010).
41. Passamonti, M., Ricci, A., Milani, L. & Ghiselli, F. Mitochondrial genomes and Doubly Uniparental Inheritance: New insights from *Musculista senhousia* sex-linked mitochondrial DNAs (Bivalvia Mytilidae). *BMC Genomics* **12**, 442 (2011).
42. Śmietanka, B., Lubośny, M., Przyłucka, A., Gérard, K. & Burzyński, A. Mitogenomics of *Perumytilus purpuratus* (Bivalvia: Mytilidae) and its implications for doubly uniparental inheritance of mitochondria. *PeerJ* **6**, e5593 (2018).
43. Breton, S. *et al.* Evidence for a fourteenth mtDNA-encoded protein in the female-transmitted mtDNA of marine mussels (Bivalvia: Mytilidae). *PLoS ONE* **6**, e19365 (2011).
44. Bettinazzi, S., Rodríguez, E., Milani, L., Blier, P. U. & Breton, S. Metabolic remodelling associated with mtDNA: Insights into the adaptive value of doubly uniparental inheritance of mitochondria. *Proc. R. Soc. B Biol. Sci.* **286**, 20182708 (2019).
45. Robin, E. D. & Wong, R. Mitochondrial DNA molecules and virtual number of mitochondria per cell in mammalian cells. *J. Cell. Physiol.* **136**, 507–513 (1988).
46. Otten, A. B. C. *et al.* Differences in strength and timing of the mtDNA bottleneck between zebrafish germline and non-germline cells. *Cell Rep.* **16**, 622–630 (2016).
47. St John, J. C. Mitochondrial DNA copy number and replication in reprogramming and differentiation. *Semin. Cell Dev. Biol.* **52**, 93–101 (2016).
48. Sano, N., Obata, M., Ooie, Y. & Komaru, A. Mitochondrial DNA copy number is maintained during spermatogenesis and in the development of male larvae to sustain the doubly uniparental inheritance of mitochondrial DNA system in the blue mussel *Mytilus galloprovincialis*. *Dev. Growth Differ.* **53**, 816–821 (2011).

49. Guerra, D., Ghiselli, F., Milani, L., Breton, S. & Passamonti, M. Early replication dynamics of sex-linked mitochondrial DNAs in the doubly uniparental inheritance species *Ruditapes philippinarum* (Bivalvia Veneridae). *Heredity* **116**, 324–332 (2016).
50. Zouros, E. Biparental inheritance through uniparental transmission: The Doubly Uniparental Inheritance (DUI) of mitochondrial DNA. *Evol. Biol.* **40**, 1–31 (2013).
51. Garrido-Ramos, M. A., Stewart, D. T., Sutherland, B. W. & Zouros, E. The distribution of male-transmitted and female-transmitted mitochondrial DNA types in somatic tissues of blue mussels: Implications for the operation of doubly uniparental inheritance of mitochondrial DNA. *Genome* **41**, 818–824 (1998).
52. Smietanka, B., Zbawicka, M., Sańko, T., Wenne, R. & Burzyński, A. Molecular population genetics of male and female mitochondrial genomes in subarctic *Mytilus trossulus*. *Mar. Biol.* **160**, 1709–1721 (2013).
53. Stewart, D. T., Kenchington, E. R., Singh, R. K. & Zouros, E. Degree of selective constraint as an explanation of the different rates of evolution of gender-specific mitochondrial DNA lineages in the mussel *Mytilus*. *Genetics* **143**, 1349–1357 (1996).
54. Śmietanka, B., Burzyński, A. & Wenne, R. Molecular population genetics of male and female mitochondrial genomes in European mussels *Mytilus*. *Mar. Biol.* **156**, 913–925 (2009).
55. Hecht, N. B., Liem, H., Kleene, K. C., Distel, R. J. & Ho, S. M. Maternal inheritance of the mouse mitochondrial genome is not mediated by a loss or gross alteration of the paternal mitochondrial DNA or by methylation of the oocyte mitochondrial DNA. *Dev. Biol.* **102**, 452–461 (1984).
56. Satoh, M. & Kuroiwa, T. Organization of multiple nucleoids and DNA molecules in mitochondria of a human cell. *Exp. Cell Res.* **196**, 137–140 (1991).
57. Obata, M., Shimizu, M., Sano, N. & Komaru, A. Maternal inheritance of mitochondrial DNA (mtDNA) in the Pacific oyster (*Crassostrea gigas*): a preliminary study using mtDNA sequence analysis with evidence of random distribution of MitoTracker-stained sperm mitochondria in fertilized eggs. *Zoolog. Sci.* **25**, 248–254 (2008).
58. Cao, L., Kenchington, E. & Zouros, E. Differential segregation patterns of sperm mitochondria in embryos of the blue mussel (*Mytilus edulis*). *Genetics* **166**, 883–894 (2004).
59. Milani, L., Ghiselli, F., Maurizii, M. G. & Passamonti, M. Doubly uniparental inheritance of mitochondria as a model system for studying germ line formation. *PLoS ONE* **6**, e28194 (2011).
60. Passamonti, M. & Plazzi, F. Doubly Uniparental Inheritance and beyond: The contribution of the Manila clam *Ruditapes philippinarum*. *J. Zool. Syst. Evolut. Res.* **58**, 529–540 (2020).
61. Ghiselli, F. *et al.* Natural heteroplasmy and mitochondrial inheritance in bivalve molluscs. *Integr. Comp. Biol.* **59**, 1016–1032 (2019).
62. Saavedra, C., Reyero, M. I. & Zouros, E. Male-dependent doubly uniparental inheritance of mitochondrial DNA and female-dependent sex-ratio in the mussel *Mytilus Galloprovincialis*. *Genetics* **145**, 1073–1082 (1997).
63. Hoarau, G., Rijnsdorp, A. D., Van Der Veer, H. W., Stam, W. T. & Olsen, J. L. Population structure of plaice (*Pleuronectes platessa* L.) in northern Europe: microsatellites revealed large-scale spatial and temporal homogeneity. *Mol. Ecol.* **11**, 1165–1176 (2002).
64. Filipowicz, M., Burzyński, A., Smietanka, B. & Wenne, R. Recombination in mitochondrial DNA of European mussels *Mytilus*. *J. Mol. Evol.* **67**, 377–388 (2008).
65. Lubośny, M. *et al.* Next generation sequencing of gonadal transcriptome suggests standard maternal inheritance of mitochondrial DNA in *Eurhomalea rufa* (Veneridae). *Mar. Genomics* **31**, 21–23 (2017).
66. MacManes, M. D. The Oyster River Protocol: a multi-assembler and kmer approach for de novo transcriptome assembly. *PeerJ* **6**, e5428 (2018).
67. Lubośny, M., Śmietanka, B., Przyłucka, A. & Burzyński, A. Highly divergent mitogenomes of *Geukensia demissa* (Bivalvia, Mytilidae) with extreme AT content. *J. Zool. Syst. Evol. Res.* **58**, 571–580 (2020).
68. Jackman, S. D. *et al.* ABySS 2.0: Resource-efficient assembly of large genomes using a Bloom filter. *Genome Res.* **27**, 768–777 (2017).
69. Dierckxsens, N., Mardulyn, P. & Smits, G. NOVOPlasty: De novo assembly of organelle genomes from whole genome data. *Nucleic Acids Res.* **45**, e18 (2017).
70. Langmead, B. & Salzberg, S. L. Fast gapped-read alignment with Bowtie 2. *Nat. Methods* **9**, 357–359 (2012).
71. Burzyński, A. & Soroka, M. Complete paternally inherited mitogenomes of two freshwater mussels *Unio pictorum* and *Sinanodonta woodiana* (Bivalvia: Unionidae). *PeerJ* **6**, e5573 (2018).
72. Badger, J. H. & Olsen, G. J. CRITICA: Coding region identification tool invoking comparative analysis. *Mol. Biol. Evol.* **16**, 512–524 (1999).
73. Birney, E., Clamp, M. & Durbin, R. GeneWise and genomewise. *Genome Res.* **14**, 988–995 (2004).
74. Delcher, A. L., Harmon, D., Kasif, S., White, O. & Salzberg, S. L. Improved microbial gene identification with GLIMMER. *Nucleic Acids Res.* **27**, 4636–4641 (1999).
75. Nawrocki, E. P. & Eddy, S. R. Infernal 1.1: 100-fold faster RNA homology searches. *Bioinformatics* **29**, 2933–2935 (2013).
76. Laslett, D. & Canbäck, B. ARWEN: A program to detect tRNA genes in metazoan mitochondrial nucleotide sequences. *Bioinformatics* **24**, 172–175 (2008).
77. Wheeler, T. J. & Eddy, S. R. nhmmer: DNA homology search with profile HMMs. *Bioinformatics* **29**, 2487–2489 (2013).
78. Käll, L., Krogh, A. & Sonnhammer, E. L. L. Advantages of combined transmembrane topology and signal peptide prediction—The Phobius web server. *Nucleic Acids Res.* **35**, W429-432 (2007).
79. Marçais, G. & Kingsford, C. A fast, lock-free approach for efficient parallel counting of occurrences of k-mers. *Bioinformatics* **27**, 764–770 (2011).
80. Zhang, N., Xu, F. & Guo, X. Genomic analysis of the Pacific oyster (*Crassostrea gigas*) reveals possible conservation of vertebrate sex determination in a mollusc. *G3 (Bethesda)* **4**, 2207–2217 (2014).
81. Zhang, G. *et al.* The oyster genome reveals stress adaptation and complexity of shell formation. *Nature* **490**, 49–54 (2012).
82. Altschul, S. F., Gish, W., Miller, W., Myers, E. W. & Lipman, D. J. Basic local alignment search tool. *J. Mol. Biol.* **215**, 403–410 (1990).
83. Untergasser, A. *et al.* Primer3—New capabilities and interfaces. *Nucleic Acids Res.* **40**, e115 (2012).
84. Lee, Y. *et al.* A mitochondrial genome phylogeny of Mytilidae (Bivalvia: Mytilida). *Mol. Phylogenet. Evol.* **139**, 106533 (2019).
85. Bouckaert, R. *et al.* BEAST 2: A software platform for Bayesian evolutionary analysis. *PLoS Comput. Biol.* **10**, e1003537 (2014).
86. Kumar, S., Stecher, G. & Tamura, K. MEGA7: Molecular evolutionary genetics analysis version 7.0 for bigger datasets. *Mol. Biol. Evol.* **33**, 1870–1874 (2016).
87. Rambaut, A., Drummond, A. J., Xie, D., Baele, G. & Suchard, M. A. Posterior summarization in Bayesian phylogenetics using tracer 17. *Syst. Biol.* **67**, 901–904 (2018).
88. Ozawa, G. *et al.* Updated mitochondrial phylogeny of Pteriomorph and Heterodont Bivalvia, including deep-sea chemosymbiotic *Bathymodiolus* mussels, vesicomyid clams and the thyasirid clam *Conchocele* cf. *bisecta*. *Mar. Genomics* **31**, 43–52 (2017).
89. Ort, B. S. & Pogson, G. H. Molecular population genetics of the male and female mitochondrial DNA molecules of the California Sea mussel, *Mytilus californianus*. *Genetics* **177**, 1087–1099 (2007).
90. Śmietanka, B. & Burzyński, A. Complete female mitochondrial genome of *Mytilus chilensis*. *Mitochondrial DNA Part B* **2**, 101–102 (2017).

91. Lee, Y.-C. & Lee, Y.-H. The F type mitochondrial genome of hard-shelled mussel: *Mytilus coruscus* (Mytiloida, Mytilidae). *Mitochondrial DNA Part DNA Mapp. Seq. Anal.* **27**, 624–625 (2016).
92. Bennett, K. F. *et al.* The F type mitochondrial genome of the scorched mussel: *Brachidontes exustus*, (Mytiloida, Mytilidae). *Mitochondrial DNA Part DNA Mapp. Seq. Anal.* **27**, 1501–1502 (2016).
93. Śmietanka, B., Wenne, R. & Burzyński, A. Complete male mitochondrial genomes of European *Mytilus edulis* mussels. *Mitochondrial DNA Part DNA Mapp. Seq. Anal.* **27**, 1634–1635 (2016).
94. Burzyński, A. & Smietanka, B. Is interlineage recombination responsible for low divergence of mitochondrial *nad3* genes in *Mytilus galloprovincialis*?. *Mol. Biol. Evol.* **26**, 1441–1445 (2009).
95. Uliano-Silva, M. *et al.* The complete mitochondrial genome of the golden mussel *Limnoperna fortunei* and comparative mitogenomics of Mytilidae. *Gene* **577**, 202–208 (2016).
96. Ranjard, L. *et al.* Complete mitochondrial genome of the green-lipped mussel, *Perna canaliculus* (Mollusca: Mytiloidea), from long nanopore sequencing reads. *Mitochondrial DNA Part B* **3**, 175–176 (2018).
97. Li, X., Wu, X. & Yu, Z. Complete mitochondrial genome of the Asian green mussel *Perna viridis* (Bivalvia, Mytilidae). *Mitochondrial DNA* **23**, 358–360 (2012).
98. Robicheau, B. M., Breton, S. & Stewart, D. T. Sequence motifs associated with paternal transmission of mitochondrial DNA in the horse mussel, *Modiolus modiolus* (Bivalvia: Mytilidae). *Gene* **605**, 32–42 (2017).
99. Sun, J. *et al.* Adaptation to deep-sea chemosynthetic environments as revealed by mussel genomes. *Nat. Ecol. Evol.* **1**, 121 (2017).
100. Uliano-Silva, M. *et al.* Complete mitochondrial genome of the brown mussel *Perna perna* (Bivalve, Mytilidae). *Mitochondrial DNA Part DNA Mapp. Seq. Anal.* **27**, 3955–3956 (2016).
101. Staden, R. The Staden sequence analysis package. *Mol. Biotechnol.* **5**, 233–241 (1996).
102. Librado, P. & Rozas, J. DnaSP v5: A software for comprehensive analysis of DNA polymorphism data. *Bioinformatics* **25**, 1451–1452 (2009).
103. Tajima, F. Statistical method for testing the neutral mutation hypothesis by DNA polymorphism. *Genetics* **123**, 585–595 (1989).

Acknowledgement

This work was supported by the Polish National Science Center (No. UMO-2015/17/N/NZ3/03538). The funders did not have a role in the study design and data collection, or the analysis, decision to publish, and preparation of the manuscript.

Author contributions

M.L, A.P., B.Ś. and A.B. designed and conceived the experiments. M.L, A.P. and B.Ś performed the experiments. M.L., A.P. and A.B. performed data analysis. M.L. and A.P. wrote the manuscript. All authors reviewed drafts of the paper and approved final manuscript.

Competing interests

The authors declare no competing interests.

Additional information

Supplementary information is available for this paper at https://doi.org/10.1038/s41598-020-67976-6.

Correspondence and requests for materials should be addressed to M.L.

Reprints and permissions information is available at www.nature.com/reprints.

Publisher's note Springer Nature remains neutral with regard to jurisdictional claims in published maps and institutional affiliations.